Ancient TL

The validity of the laboratory reconstruction of palaeodose

G. Hütt[†] and J. Jaek[§]
[†]Institute of Geology, Estonia pst. 7, Tallinn 200101, USSR
[§]Tartu State University, Tähe 4, Tartu 202400, USSR

Introduction

The problem of laboratory reconstruction of palaeodose is common to all the palaeodosimetry dating methods (TL, OSL, ESR). It is known that the quartz TL dose response curve, obtained using β and γ laboratory sources, can be represented by a multi-stage process, as shown in figure 1:

Stage I may be explained by competition between traps with different effective cross sections which are empty at the initial moment of irradiation;

Stage II is characterised by the filling of existing defects (traps) by charge carriers;

Stage III corresponds to saturation, where all the existing traps are filled;

Stage IV represents the generation and filling of new defects.

The fourth stage is simultaneous with the second one, but due to its lower efficiency it becomes apparent only after the stage of saturation. The accumulated dose at which the fourth stage is observed has not been fixed since it depends on the number of traps in the palaeodosemeter, i.e. on the second and third stages.

However, in nature the dose rate is several orders of magnitude lower than that used in the laboratory and the validity of the assumption that the growth characteristics are similar for the two situations has been considered previously (eg Aitken, 1985, p.1412). The essence of the problem is that in case of low natural dose rates saturation may be reached, not as a result of a shortage of traps, but due to thermodynamic equilibrium between the input and output of trapped charge carriers. In this case the values of laboratory and natural saturation levels may be different if the lifetime of charge carriers in traps is not sufficiently long. The implication of such a difference is, in principle, that the saturation value (the second stage) will depend on dose rate.

Experiments with CaF_2 (Aitken, 1985, p141) have shown that saturation TL values do not change if the laboratory dose varies from 0.3 mGy/min to 3 Gy/min. However, changes may have taken place at considerably lower dose rates where it is impossible to model experimentally a situation close to the natural one. Consequently the level of dose at which the dependence on dose-rate for traps with trapped charge mean lifetimes comparable with dating timescales becomes significant may be within the regime of accrued palaeodose for dating samples.

The first results indicating a possible difference between natural palaeodose formation and its laboratory reconstruction were obtained from the TL dating of loess sections. In spite of the absence of saturation under laboratory conditions, no ages greater than 100 ka were obtained (Debenham, 1985). In previous work (by G.H.) on loess of ages ranging from the contemporary to 1.5 Ma, it had been found that TL ages greater than 30 ka were systematically younger than reliable geological estimates. These results suggest that the apparent limits of the TL method may vary according to geographic location and that these limits are considerably lower than those predicted by the laboratory dose response results. The accuracy of the dates obtained remains topical as well.

Shljukov and Shakovets (1986), after attempting to reconstruct palaeodose by means of X-ray sources of radiation with a dose rate 30 Gy/min. concluded that laboratory calibration was not a valid procedure. They also assumed the natural saturation value for quartz to be constant for all geological regions.

Model for palaeodose formation and age correction

Vagn Mejdahl (1988) discovered a difference between natural and laboratory saturation for alkali feldspars from one of the regions and took it to be a common phenomenon related to long term fading. He suggested the correction of dates in view of the discrepancy between the values of natural and laboratory saturation.

In this paper a further method for the correction of dates is presented, based on a consideration of differences between natural and laboratory saturation values. We leave aside the agents accounting for this discrepancy: in complex many-impurity system losses may take place during such a long term period due to non-radiative transmission, redistribution of charge carriers, diffusion etc. In the case of fine grains (4-11 μm), competition between surface and volume defects (Kortov, 1986) may partly account for this effect.

The proposed model permits the evaluation of the critical dose rate, i.e. the minimal dose rate at which the above mentioned dependence is negligible, but also the effective lifetime of change carriers in the traps. The correction formula is based, not on formal rules, but on actual processes of palaeodose formation which enables experimental parameters to be used. Only stages II and III of the dose response curve (figure 1) are considered.

Palaeodose formation is a monomolecular process, and, unlike the optical bleaching process, the elucidation of its order of kinetics requires special experiments. The main kinetic formula of palaeodose formation is as follows:

$$\frac{dn}{dt} = \beta(N - n) - \alpha n \tag{1}$$

where,

$\frac{dn}{dt}$ is the number of electrons stored per unit time

N - the total number of traps of the type considered

n - number of traps occupied at time t

α - probability for carriers to escape from traps

β - probability of capture for electrons from the conduction band

$$\frac{1}{\tau} = \alpha = P_o \, e^{-E/kT} \tag{2}$$

where,

τ - is the life time of carriers in the trap

E - trap thermal activation energy

P_o - frequency factor

k - Boltzmann's coefficient

T - storage temperature

Solving the differential equation (1),

$$dt = \frac{\alpha n}{\beta N - n(\alpha + \beta)} \tag{3}$$

$$\frac{-1}{\alpha + \beta} \ln [\beta N - n(\alpha + \beta)] = t + \ln C \tag{4}$$

$$\ln C = \frac{-1}{\alpha + \beta} \ln \beta N \tag{5}$$

$$t = \frac{-1}{\alpha + \beta} \ln \frac{\beta N}{\beta N - (\alpha + \beta)n} \tag{6}$$

For saturation, $n \rightarrow n_\infty$, $\frac{dn}{dt} = 0$

Equation (1) yields

$$\beta N - n_\infty (\alpha + \beta) = 0 \tag{7}$$

$$\alpha + \beta = \frac{\beta N}{n_\infty} \tag{8}$$

Substituting (8) in (6),

$$t = \frac{n_\infty}{\beta N} \ln \frac{\beta N}{\beta N - \frac{\beta N}{n_\infty} n} \tag{9}$$

$$t = \frac{n_\infty}{\beta N} \ln \frac{1}{1 - \frac{n}{n_\infty}} \tag{10}$$

Introducing βN, the probability of capture with unoccupied traps, and γ, the dose sensitivity at the linear stage of the dose response curve, the following formula may be defined,

$$\beta N = \gamma P \tag{11}$$

where P is the dose rate, $\frac{dD}{dt}$.

From equations (11) and (10),

$$t = \frac{n_\infty}{\gamma P} \ln \frac{1}{1 - \frac{n}{n_\infty}} \tag{12}$$

Initially $(N \gg n_0)$ there are many more unoccupied traps than charge carriers and the change in the number of charge carriers in the traps is determined by the dose sensitivity.

Putting γ, the change in the number of trapped charge carriers per unit laboratory dose, into (12),

$$t = \frac{n_\infty dD}{dn_0 P} \ln \frac{1}{1 - \frac{n}{n_\infty}} \tag{13}$$

n_∞ may be realised both at the natural $(n_{\infty N})$ and the laboratory dose rate $(n_{\infty L})$.

Assuming,

t_1 - age corresponding to the palaeodose induced by the natural radiation

t_2 - age corresponding to the palaeodose reconstructed by laboratory irradiation

we get from (10),

$$t_1 = t_2 \frac{n_{\infty N}}{n_{\infty L}} \left(\ln \frac{1}{1 - \frac{n}{n_{\infty N}}} \right) \cdot \left(\ln \frac{1}{1 - \frac{n}{n_{\infty L}}} \right)^{-1} \tag{14}$$

For correction, the natural saturation level, $n_{\infty N}$, must be known i.e. using samples with ages beyond the limits of the method.

Dependence of saturation value on dose rate

As was shown above, the model enables the dependence of saturation value on dose rate to be established for traps with different trapped charge carrier life times. Using formula (8) it is possible to determine the number of trapped charge carriers in the saturation stage.

$$n_\infty = \frac{\beta N}{\alpha + \beta} \tag{15}$$

It is worth noting here that β is the probability for electrons located in the conduction band to be captured in vacant traps and consequently must depend on dose-rate. From (11) and (15),

$$n_\infty = \frac{P\gamma}{\alpha + \beta} \tag{16}$$

If there are two dose rates, P_1 and P_2, corresponding to two different saturation values $n_{1\infty}$ and $n_{2\infty}$ respectively, and assuming γ is constant, we obtain

$$\frac{n_{1\infty}}{n_{2\infty}} = \frac{P_1(\alpha + \beta_2)}{P_2(\alpha + \beta_1)} \qquad (17)$$

If storage takes place in shallow traps (ie $\alpha \gg \beta$) and neglecting β, (17) may be written as,

$$\frac{n_{1\infty}}{n_{2\infty}} = \frac{P_1}{P_2} \qquad (18)$$

which shows that for shallow traps (τ is small) the saturation value is proportional to dose-rate. For deep traps ($\alpha \ll \beta$) with sufficiently long charge carrier lifetimes, substituting in (19) the expression for β obtained from (11) gives,

$$\frac{n_{1\infty}}{n_{2\infty}} = \frac{P_1 \dfrac{\gamma P_2}{N}}{P_2 \dfrac{\gamma P_1}{N}} = 1 \qquad (19)$$

Dose rate dependence of n_∞ is not observed with deep traps. The proposed model enables the estimation of the values of dose rate at which the probabilities of trapping and eviction of charge carriers from a particular trap are of the same magnitude (potential equilibrium conditions).

If we assume $\alpha = \beta$, and as in the laboratory saturation stage all the vacant traps are filled, i.e. $N = n_{\infty_L}$, formula (11) may be rewritten in the following way:

$$\beta = \frac{\gamma P}{n_{\infty_L}} \qquad (20)$$

As γ is the palaeodosimetry dose sensitivity, $\dfrac{dn_o}{dD}$, and, in this case $\beta = \alpha = 1/\tau$, then,

$$\frac{1}{\tau} = \frac{dn_o\, P_{crit}}{dD\, n_{\infty_L}} \qquad (21)$$

$$P_{crit} = \frac{dD\, n_{\infty_L}}{dn_o \tau} \qquad (22)$$

The critical dose rate value for traps with different life times may be calculated from formula (22) when τ is known.

The model presented furnishes a basis for estimating effective lifetimes, τ_r, of charge carriers in traps considering the difference between natural and laboratory saturation values. Leaving aside mathematical calculations, we confine ourselves with presenting the final formula only:

$$\tau_r = \frac{dD\, n_{\infty_L}}{dn_o\, P_N}\left(\frac{n_{\infty_L}}{n_{\infty_N}} - 1\right) \qquad (23)$$

where,

τ_r - is the effective lifetime of charge carriers in traps valid for individual samples in natural conditions of burial.

Below is a table of age correction coefficients obtained from laboratory reconstruction of palaeodose.

Table 1. Age correction coefficients for laboratory reconstruction of palaeodose.

$\dfrac{I_N}{I_{\infty_N}}$	$I_{\infty_L}/I_{\infty_N}$						
	1.1	1.2	1.5	2	3	5	10
10	1.002	1.005	1.03	1.04	1.04	1.04	1.05
25	1.015	1.03	1.06	1.09	1.10	1.12	1.18
50	1.033	1.06	1.15	1.23	1.26	1.31	1.38
75	1.10	1.17	1.33	1.46	1.61	1.69	1.78
90	1.23	1.38	1.57	1.72	1.90	2.32	2.45
99	1.82	2.20	2.78	3.33	3.38	4.18	4.42

Discussion

The main problem is the determination of the natural saturation value (I_{∞_N}) to get the ratio $I_{\infty_L}/I_{\infty_N}$. Laboratory and natural saturation values have been found to be equal equal ($I_{\infty_L}/I_{\infty_N} = 1$) for numerous quartz samples from different climatic regions. For each sample, added laboratory doses did not result in an increase in TL, from which we conclude that the laboratory saturation value had been obtained.

As discussed above, laboratory and natural saturation values are functions of the number of traps, but the latter additionally depends on τ of the corresponding traps. τ for the relevant traps in quartz is $\sim 10^{13}$ a, assuming a monomolecular model (Hütt et al., 1979), and this accounts for the similarity of the laboratory and natural saturation values. Consequently, the laboratory reconstructed palaeodose needs no correction. In the case of other materials (feldspars, carbonates), the problem is more complicated. Investigations (Mejdahl, 1988; and our results using OSL) of old samples have shown that for alkali feldspars the laboratory saturation value is greater than the natural saturation value. Consequently for dating samples, the theoretical value, $\tau = 3.10^7$ a, is not realised for a quasi-continuous energy trap spectrum (Strickertsson, 1985) of alkali feldspars, and generally a much lower value applies.

The difference between natural and laboratory saturation values was measured by ESR for aragonite shells (Hütt and Jaek, in press). The important problem of constancy of the natural saturation level, independent of the geological region of sampling, needs additional investigation for old samples from different climatic regions. If processes of age information "degradation" are thermally dependent, this value will be constant only for definite climatic regions. In cases where these processes are not

strongly thermally dependent (like non-radiative transitions) this ratio may be effectively constant.

As an illustration of usage of the proposed model we analysed an experimental dose response curve for alkali feldspars from a marine sediment sample to estimate P_{crit} and τ_n (see equations 22, 23). Using the following values; $\Delta D = 300$ Gy; $\Delta I = 171$, $I_{\infty_L} = 896$, $I_{\infty_L}/I_{\infty_N} = 1.2$ (pers. comm. Vagn Mejdahl, 1988) yields

$$P_{crit} = 5.25.10^{-5} \text{ Gy a}^{-1} \qquad \tau = 3 \times 10^6 \text{ a}$$

The fact that P_{crit} is two orders of magnitudes smaller than the annual dose rate $(2.5.10^{-3} \text{ Gy.a}^{-1})$ demonstrates that dependency of saturation value dependency on dose rate is absent within the range from natural to laboratory rates. However, the effective thermal stability of carriers in the particular traps confirms Mejdahl's conclusion that the upper limits of dating are lower than values deduced from laboratory reconstructed dose response curves.

Conclusion

1. The standard plateau test is a necessary but insufficient condition for obtaining reliable results.

2. The saturation test is not valid for alkali feldspars, carbonates and, perhaps, other minerals, because the growth of signal may be observed for naturally saturated samples too.

3. The fact that $I_{\infty_L}/I_{\infty_N} > 1$ decreases the upper dating limit requires corrections to be applied to TL dates.

4. Experimental studies of samples having ages beyond the dating limits from wider climatic regions are necessary.

References
Aitken, M. J. (1985) *Thermoluminescence dating*. Academic Press, London.

Debenham, N.C. (1985) Use of U.V. emissions in TL dating of sediments, *Nucl. Tracks and Radn. Measts.*, **10**, 717-725.

Hütt, G., Smirnov, A. and Tale, I., (1979), On the application of TL of natural quartz to the study of geochronology of sedimentary deposits, *PACT J.*, **3**, 362-374.

Hütt, G., and Jaek, I., Laboratory reconstruction of palaeodose: problems of dating accuracy and upper limitation, *Appl. Rad. and Isotopes*, in press.

Kortov, V.C., (1986), radiation defects on the surface of silica and aluminium oxides crystals, Abstracts, The VI All Union Conference on Radiation Physics and Chemistry of Ion Crystals, Riga, Oct 9-11, 1986, (in Russian), 27.

Mejdahl, V., (1988), Long term stability of the TL signal in alkali feldspars, *Quarternary Science Reviews*, **7**, 357-360.

Shljukov, A., and Shakhovets, S. (1986), The validity of radiation calibration of quartz in TL dating, International TL Workshop on Methodology of TL Dating, Tallinn, April 20-24, 2986. (Unpublished).

Strickertsson, K., (1985), The thermoluminescence of potassium feldspars, *Nucl. Tracks and Radn. Measts.*, **10**, 613-617.

PR Reviewer's comments (Vagn Mejdahl)
The use and definition of the term critical dose-rate might benefit from some reconsideration. As the natural dose-rate is increased, the saturation level will gradually approach the laboratory saturation level, and it becomes a matter of definition when the natural dose-rate is sufficiently high for the application of a fading correction to be no longer required. Thus the concept and evaluation of a "critical" step in this situation appears inappropriate.
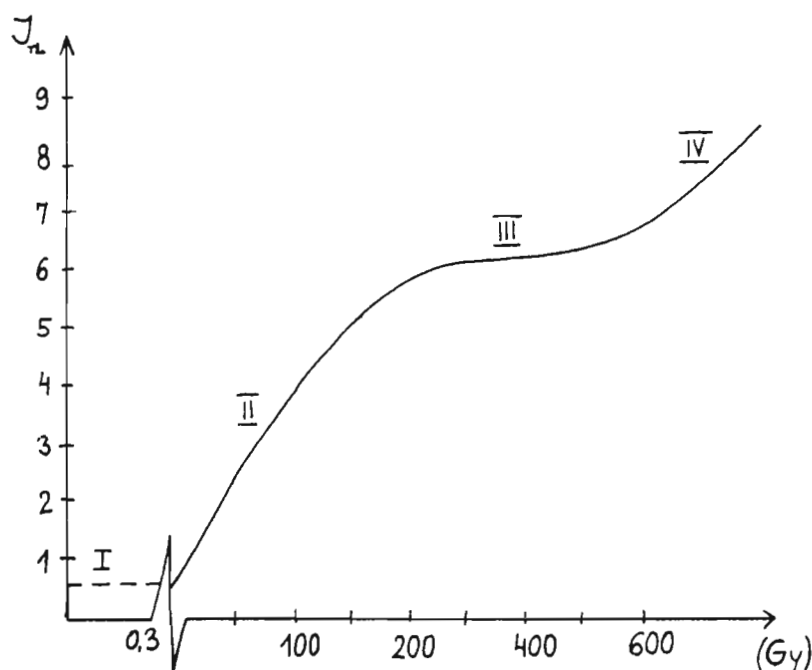

Figure 1. Dose response curve. Axes; the ordinate represents TL signal (arb. units), and the abscissa represents laboratory dose (Gy).

Treatment of error in plateau values - caveat emptor

Glenn W. Berger [†] and D. J. Huntley [§]

[†] Department of Geology, Western Washington University, Bellingham, WA 98225, U.S.A.
[§] Department of Physics, Simon Fraser University, Burnaby, B.C. V5A 1S6, Canada

Introduction

The treatment of the estimated errors in the equivalent-dose (D_e) values in plateau plots appears to have sometimes been handled incorrectly in recent publications. We discuss here what the correct treatment should be. We raise this subject because of an earlier instance (Rendell, 1985) in which some mathematical expressions ascribed to us were incorrectly quoted, and because we suspect that there is here a new misuse of some expressions which originated with us. We wish to re-emphasize the dangers of using any programs for which one does not understand the limitations of the mathematical routines.

Discussion of different ways to assess plateau values has also been a part of the development of more mature dating methods (e.g. Berger and York 1981). Hence, this matter should be clarified now before unnecessary differences in interpretation of TL dates arise. Specifically, some results [eg Forman, 1988; Forman et al. 1988, some of the Alpha Analytic dates (private communication)] present errors in the mean D_e values (hence in the TL age estimates) that are unrealistically small, by a factor of two to ten. Most of the data of Forman et al. (1988) are reproduced (with some puzzling differences in cited errors) in Forman et al. (1989), but in the latter case the single D_e plot does not reveal any discrepancy in error assignment.

We are not singling out Forman and colleagues for mischievous reasons, but only because they have been careful enough to publish examples of growth curves and/or plots of equivalent-dose plateaus which enable us to draw inferences about their treatment of errors. We are distressed at the number of authors who do not publish such plots (and the editors and reviewers who allow this omission). Presently, statistical treatments of errors in TL data for sediments (young or old) cannot be judged objectively by independent workers without such plots. As a corollory, mere tabulation of TL dates (e.g. Drozdowski and Fedorowicz 1987, Zöller et al. 1988, Zubakov et al. 1988) has little value. In fact, few of the sediment TL dates yet published satisfy all the criteria for acceptability proposed by Wintle and Huntley (1982).

Two types of error estimate

There appear to be two kinds of error estimate in circulation. This supposition is made because one of us (GWB) wrote the early error routines for the TL laboratory at Cambridge and the now-defunct commercial Alpha Analytic laboratory in Miami, Florida. These routines contained two error estimates: the first, the average of the individual D_e error estimates; the second, the weighted error of the mean.

This second estimate is calculated using a weighting appropriate for the case in which all the individual errors are statistically uncorrelated (often referred to as the standard error of the mean, e.g. Topping 1962). This second estimate is always smaller than the first and would be appropriate only if the errors were due entirely to, for example, photon-counting statistics. The "correct" error estimate will normally lie somewhere between these two extremes, but in practice is usually closer to the larger first estimate, because the errors in the individual D_e values are highly correlated. A proper calculation requires a knowledge of the covariance terms of the errors in the individual D_e values, but these covariance terms are not known.

What is the evidence that the errors in the individual D_e values are usually highly correlated? These errors reflect the scatter of the glow curves -- their reproducibility, manifesting largely subsample variability. Almost always, when one glow curve is lower or higher than another, this difference not surprisingly persists over several channel or temperature points (as much as 50-100 °C). This shows up on a D_e vs T plot as a sequence of D_e values which have much less scatter than expected on the basis of the size of the error bars on the individual points.

Errors in individual D_e values will likely be uncorrelated only when the "noise" in each glow curve is dominated by photon-counting statistics or some instrumental characteristic. Such glow curves commonly are observed when the signal intensity is very low (less than a few hundred photon-counts per channel), such as for very young volcanic ash samples. Use of the standard-error-of-the-mean estimate is warranted only in such cases of very low photon counts.

Figure 1 shows two equivalent-dose plots of real data which illustrate the two situations described above. Part A represents a 500 year-old tephra which had low TL signals, whereas part B represents a $\approx 40,000$ year-old lake sediment. For the former, the standard-error-of-the-mean error estimate is appropriate, whereas for the latter the average error is valid.

The use of integral D_e determinations (that is, calculated from TL data integrated over a broad region of the glow curves) might seem to be a useful way to reduce the error in the final D_e value, but a little thought and an example show that this approach provides no advantage. Consideration of fig 1a and the underlying glow curves (Berger and Huntley, 1983) shows that an integral D_e will reduce the error to the same extent as the weighted error of the mean, without having the benefit of a plateau test. Consideration of fig. 1b reveals that an integral D_e will yield the same error as the average of the individual errors in the plateau. We have done this calculation for the TL data underlying fig 1b and verified that this is so. These results are not suprising, given the main reasons for correlation (or not) of errors (discussed above). A final argument against the use of an integral calculation is that it side-steps use of a proper plateau test. Many workers use only the simplistic ratio-of-glow-curves method for a plateau test and follow this with an integral calculation. This approach is inadequate for it depends on the assumption of a linear dose response for all samples and all regions of the glow curves.

A practical example

There is also a practical way to determine which of the two error estimates is appropriate. One can simply repeat the equivalent-dose experiment several times on a given sample. Various levels of care could be used. Perhaps the most realistic approach would be to do each experiment on a separately prepared set of discs for a given sample. In this way the variability between disc sets could be factored into the estimate of error in the plateau D_e value. This approach is certainly the most realistic if one expects to compare error estimates in TL dates between different laboratories, or indeed between different samples. Of course if one has such replicate data, one can use the results with proper statistical weighting to produce a better error estimate than is represented by any individual result.

To our knowledge, this experiment has not yet been done using the partial-bleach or regeneration techniques. If anyone has done such experiments, we would be interested to hear of the results. However, such an experiment has been done using the additive-dose technique applied to the Mazama volcanic ash (Berger and Huntley, 1983). To support our arguments and to provide convenient access to these results, we reproduce in Table 1 here some of these data for the Mazama ash. These data show that the most realistic error estimate for the plateau D_e is the average error over the plateau region . The smaller

weighted- error-of-the-mean estimate does not reflect the actual reproducibility of the plateau experiments.

Conclusion

In the absence of a statistically correct procedure for evaluating the error in the quoted D_e, the best estimate of this error will usually be obtained by taking the average (over the plateau) of the errors in the individual D_e values. This may be an overestimate in some cases, but that is not nearly as serious a mistake as making a large underestimate.

Table 1.   Repeat equivalent-dose measurments for Mazama ash

D_e (Gy)	Ave. error (Gy)	
25.9	0.9	average = 27.9
26.9	1.0	
28.9	1.8	standard deviation = 1.7
26.4	2.6	
30.4	2.0	standard error
28.7	2.2	of the mean = 0.7

References

Berger, G. W. and York, D. (1981) Geo-thermometry from $^{40}Ar/^{39}Ar$ dating experiments. *Geochim. Cosmochim. Acta.,* **45**, 795-811.

Berger, G. W. and Huntley, D. J. (1983). Dating volcanic ash by thermoluminescence. *PACT J.,* **9**, 581-592.

Drozdowski, E. and Fedorowicz, S. (1987) Stratigraphy of Vistulian glaciogenic deposits and corresponding thermoluminescence dates in the lower Vistula region, northern Poland. *Boreas,* **16**, 139-153.

Forman, S.L. (1988) The solar resetting of thermoluminescence of sediments in a glacier-dominated fiord environment in Spitsbergen: geochronologic implications. Artic and Alpine Research, **20**, 243-253.

Forman, S. L., Jackson, M. E., McCalpin, J. and Maat, P. (1988) The potential of using thermoluminescence to date buried soils developed on colluvial and fluvial sediments from Utah and Colorado, U.S.A.: preliminary results. *Quat. Sci. Rev.,* **7**, 287-294.

Forman, S. L., Machette, M. N., Jackson, M. E. and Matt, Paula. (1989) An evaluation of thermoluminescence dating of paleoearthquakes on the American Fork segment, Wasatch Fault zone, Utah. *J. Geophys. Res.,* **94**, 1622-1630.

Rendell, H. M. (1985) Problems with linear regression as applied to TL data. *Ancient TL,* **3**, 6-9.

Topping, J. (1962) Errors of observation and their treatment. Chapman and Hall.

Wintle, A. G. and Huntley, D. J. (1982) Thermoluminescence dating of sediments. *Quat. Sci. Rev.,* **1**, 31-53.

Zöller, L., Stremme, H. and Wagner, G. A. (1988) Thermolumineszenz-datierung an löss paläo-boden-sequenzen von nieder-, mittel- und oberrhein/Bundesrepublik Deutschland. *Isotope Geology,* **73**, 39-62.

Zubakov, V. A. (1988) Climatostratigraphic schemes of the Black Sea Pleistocene and its correlation with the oxygen-isotope scale and glacial events. *Quaternary Research,* **29**, 1 - 24.

P.R. Reviewer's comments (Rainer Grün)
This is a very timely comment on error treatment in
TL dating. It would be of great value if the authors also
commented on the general validity of linear fits, and
whether it would be more realistic to use integral ED
determinations. This leads, of course, to the general
discussion of whether the existence of signal and ED
plateaux are sufficient criteria for the reliable evaluation
of the ED.

Reply
In this paper we have attempted to address a small but
significant computational aspect concerning D_e
determination and not the broader issues raised by the
Reviewer. However, a more detailed discussion of curve
fitting may be found in Berger et al (Berger, Lockhart
and Kuo, 1987); the plateau test is not a sufficient
condition for the validity of D_e, but as Aitken (1985)
has pointed out previously, it is certainly necessary.
Part of the problem of the development of the TL
dating methods has been the over-zealous interpretation
of "something flat" as a chronologically meaningful
parameter.

Reference

Berger, G.W., Lockhart, R.A., and Kuo, J. (1987)
    Regression and error analysis applied to the dose-
    response curves in thermoluminescence dating.
    Nucl. Tracks and Radn. Measts., **13**,177-184.
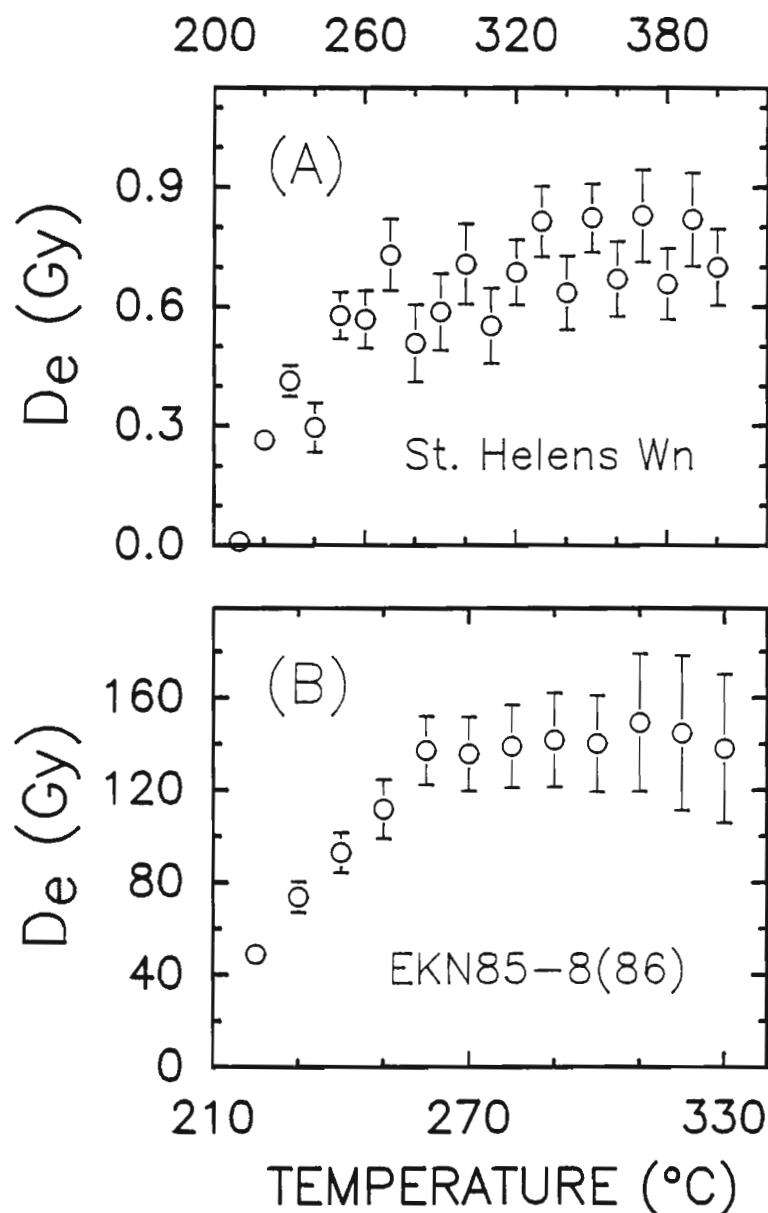

Figure 1.
*Equivalent-dose plots for two sets of data, representing the situations of highly uncorrelated (A) and highly correlated (B)
errors in individual D_e values. The data of part A represent additive-dose results for the Mt. St. Helens Wn tephra from
Berger and Huntley (1983), whereas the data of B represent partial-bleach (R - β) results of Berger (unpublished).*

Significant peak enhancement of the natural TL signal observed after short term storage at 75 °C

M.L. Clarke[†] and A.G. Wintle[§]

[†] Department of Geography, University of Leicester, University Road, Leicester, LE1 7RH.
[§] Institute of Earth Studies, University College of Wales, Aberystwyth, Dyfed, SY23 3DB.

Introduction
Loess samples found to exhibit anomalous fading have, in the past, been subject to inconveniently long post-irradiation storage periods to await complete removal of the unstable TL component. Various pre-heat procedures have been developed, following experimental studies on zircon by Templer (1985), and they have been critically discussed by Berger (1988). Berger (1987) has reported that storage of up to 8 days at an elevated temperature of 75 °C removes the unstable signal equivalent to 160 days at room temperature. This paper describes a series of measurements in which the natural TL signal exhibited a significant peak enhancement of up to 36% over a period of 1-8 days relative to the natural TL signal stored at room temperature (25 °C). Obviously a temperature-induced sensitivity change has serious implications for reliable dating.

Experimental observations
Polymineral fine-grain loess samples from Gold Hill, near Fairbanks, Alaska, were found to exhibit severe anomalous fading at room temperature. Fading has previously been reported in Alaskan loess samples from Halfway House (Berger, 1987), within 10km of the Gold Hill locality. Fading in the Gold Hill samples was observed in the green region of the spectrum with a Corion S40-550 band pass filter, whereas. Berger (1987) looked at the TL emission in the blue part of the spectrum using a Corning 5-58 filter. The occurrence of anomalous fading in both the blue and the green emissions implies that fading is not related to a specific luminescence centre.

As Berger (1987) had proposed that short-term storage periods of up to 8 days at 75fC removed a large proportion of the unstable TL component, a series of measurements were carried out on discs left at 75 °C for 1-8 days prior to glowing. An equivalent set of discs were left at room temperature (25 °C) for the same period. The discs were glowed immediately after storage with the entire experiment repeated in three different spectral regions (UV, blue and green) using a Daybreak Bandpass Filter System. The filters used were a Schott UG11 combined with a BG38 (UV), a Corion S40-400 (blue) and a Corion S40-550 (green). The choice of filters was determined with reference to the emission spectrum obtained by Huntley et.al. (1988) on a sample of Alaskan loess from the Fairbanks area. The principle emissions occurred in the blue and green region.

Surprisingly, none of the irradiated discs showed any significant fading after storage at 75 °C. However, the natural TL discs exhibited a marked peak enhancement, of up to 36% over 1, 2, 4 and 8 day periods at 75 °C with respect to those at 25 °C. This enhancement occurred over the entire glow curve suggesting that it is not a function of trap depth (figure 1). It was visible with all three filters and with four different samples.

Further experiments were then conducted to test whether the natural signal from Alaskan loess was therefore temperature dependent. Discs were glowed immediately after being taken from an oven where they had been stored for intervals of 1, 2, 4 and 8 days at various temperatures ranging from -15 °C to +110 °C. Only the natural discs left at 75 °C showed an increase in signal intensity. The natural glow curves for the other temperatures were identical to those at 25 °C, except for those held at temperatures above 90 °C which exhibited a slight loss of signal on the lower temperature side of the glow curve.

The enhanced natural TL signal was also found to be relatively unstable, in that leaving the natural discs at 75 °C for 1 day and then for 18 hours at room temperature prior to glowing causes the enhanced signal to decay back to its original (room temperature) level.

The effect of such a signal enhancement on calculation of the ED was tested by substituting the natural response at 75 °C into a set of regeneration data from the same sample left at room temperature. The ED obtained at room temperature with the original data was 60 Gy; however, by substituting just the naturals with the peak enhanced signal the ED obtained was 138 Gy. Obviously an apparent increase of 78 Gy has serious implications for dating by the regeneration method. Such problems are unlikely to be encountered by the total- or partial-bleach methods (as used by Berger, 1987) because of the delay imposed by subsequent optical bleaching procedures.

Conclusions
Although the behaviour exhibited by these samples is difficult to understand and interpret, the possible implications are serious enough to warrant further investigation. The lack of fading observed for irradiated

samples stored at 75 °C may be due to the enhanced signal cancelling out the decrease caused by fading over the 8 day period. It is clear that readout immediately after storage at 75 °C will lead to erroneous results and at least 24 hours should pass before the glow curves are measured. Such a precaution was taken by Berger (1987) as evidenced by data in figure 2 of his paper; he also stated that the TL from unirradiated sub-samples was unaffected by storage intervals of up to 8 days at 75 °C.

References

Berger, G.W. (1987) Thermoluminescence dating of the Pleistocene Old Crow tephra and adjacent loess, near Fairbanks, Alaska, *Canadian Journal of Earth Sciences,* **24**, 1975-1988.

Berger, G.W. (1988) Dating Quaternary events by luminescence, Geological Society of America, Special Paper 227, 13-50.

Huntley, D.J., Godfrey-Smith, D.I., Thewalt, M.L.W. and Berger, G.W. (1988) Thermoluminescence spectra of some minerals relevant to thermo-luminescence dating, *Journal of Luminescence,* **39**, 123-126.

Templer, R.H. (1985) The removal of anomalous fading in zircon, *Nuclear Tracks and Radn Measts,* **10**, 531-537.

PR Reviewed by Glenn Berger

Schott UG11 and BG38.
UV emission
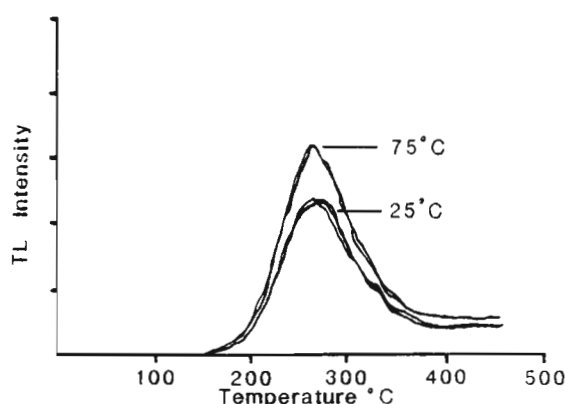
Corion S40-400.
Blue emission
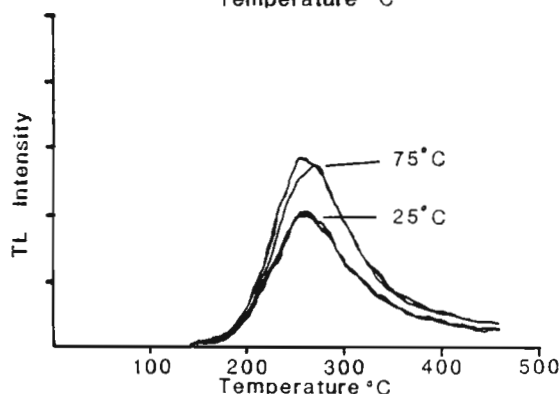
Corion S40-550.
Green emission
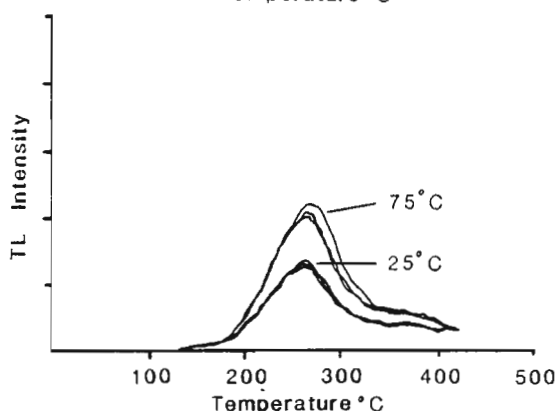
Figure 1.
Glow curves obtained from natural discs of sample GHC27 using three different colour filters. The discs were glowed after one day storage period. The natural glow curves for temperatures ranging from - 15 °C to +110 °C were identical to those at 25 °C, except that those held at temperatures above 90 °C exhibited a slight loss of signal on the lower temperature side of the glow curve.

Ranges of alpha particles in various media

B.J. Brennan [†] and R.G. Lyons [§]
Departments of [†]Physics and [§]Geography, University of Auckland, New Zealand

It is now well established that the TL or ESR signal induced by an alpha particle is very nearly proportional to its range (Aitken and Bowman, 1975; Lyons, 1988; Lyons and Brennan, 1989a, 1989b). Knowledge of the variation of alpha particle range with energy is thus important to the estimation of the alpha particle contribution to the environmental dose rate for samples used in ESR and TL dating. Zimmerman (1971) used data on ranges in aluminium from Marion and Young (1968) to infer ranges in ceramics, while interpolations between neon and sodium in the tabulations of Northcliffe and Schilling (1970) and Williamson et al. (1966) were used by Aitken and Bowman (1975) to estimate ranges in pottery. A later tabulation by Zeigler (1977) has been employed by Lyons and Brennan (1989a, 1989b) to estimate ranges in calcite, and by Valladas (1988) to tabulate stopping powers and ranges in silica.

A more recent volume by Zeigler et al. (1985) provides a data set which is a development of the work of Zeigler (1977) and companion volumes relating to heavy ions other than alpha particles. Because the 1985 volume employs a more complete and recent set of experimental data together with improvements in the calculation techniques employed, the results are more reliable than the 1977 volume and earlier tabulations referred to above. Zeigler and his co-workers make available computer software for the calculation of ranges and stopping powers and Monte-Carlo simulation of target penetration by heavy ions. The software is updated continuously and the most recent (1988) version is written in TURBO-BASIC for an IBM-PC or compatible computer.

In this paper we present the results of calculations employing the software provided by Zeigler and his co-workers. We used the implementation of the PRAL transport equation to calculate average projected ranges (that is, distance traveled in the original direction of motion) for alpha particles in the various media. While it might be argued that the total path length is the fundamental determinant of ionization damage and thus ESR or TL signal for an alpha particle, the difference between total and projected path length is less than 1% for energies of 1 Mev or greater; and in addition the projected path length is fundamental to estimation of dose due to sources external to a sample. In Zeigler's 1988 computer program, the stopping power of the target is calculated as the appropriately weighted sum of the stopping powers of the constituent elements, and bonding corrections can be made for some bonds involving light elements. Nuclear as well as electronic stopping effects are including. The stopping powers for carbon and oxygen in solids have been used. Base data for stopping powers is in units of $eV/(1 \times 10^{15}$ molecules $cm^{-2})$, but range data is presented here in mg cm^{-2} for ease of comparison.

The compositions used for the various materials are given in table 1. As Zeigler's software accepts no more than 6 elements, it was sometimes necessary to combine some of the lower concentration elements with others of similar atomic number e.g. aluminium and magnesium, potassium and calcium. Note that most materials which are commonly used in ESR or TL dating have similar effective atomic masses (A_{av}) and charges (Z_{av}) with the result that their ranges are very similar if measured in mg cm^{-2} (fig. 1). The most notable exception is bone, which has a much lower effective atomic mass and charge due to the high proportion of hydrogen and carbon, and hence shorter ranges. Silica and dry pottery represent the extremes for the remaining dating materials, with the majority lying closer to silica than to pottery.

While the difference between some materials may not be significant in a particular application, all the data sets are included in table 2 for completeness as they represent the most up-to-date information available; it is left to the user to assess the degree of accuracy required. For simplicity of presentation the corresponding stopping powers are not tabulated here; they may be derived from Zeigler's software or from the equations in table 3. Alternatively, we would be pleased to supply them and/or more details of range data on request.

From the values given in table 2 the ranges for other energies may be readily obtained by interpolation using, for example, a cubic spline. Alternatively, ranges for each compound may be generated using the cubic polynomials for range as a function of energy given in table 3. These polynomials were obtained by a least squares fit to 80 range data points which were approximately logarithmically distributed between 10 keV and 10 MeV, and are accurate to within 0.01 mg cm^{-2} for ranges up to 10 MeV. The differential with respect to energy (dR/dE) gives quadratics from which ranges and stopping powers (dE/dR) may be

Table 1. Ranges in mg cm^{-2} for alpha particles of different energies (MeV) for dating materials:

a) simple

Energy	CaCO$_3$	SiO$_2$	Albite	Orthoclase	Anorthite	Al
0.01	0.026	0.027	0.027	0.027	0.027	0.027
0.05	0.096	0.098	0.098	0.100	0.100	0.101
0.10	0.155	0.156	0.155	0.160	0.159	0.160
0.15	0.203	0.201	0.200	0.206	0.206	0.209
0.2	0.245	0.241	0.240	0.247	0.248	0.254
0.3	0.322	0.311	0.311	0.319	0.323	0.337
0.4	0.391	0.374	0.376	0.385	0.392	0.418
0.6	0.519	0.495	0.500	0.511	0.522	0.576
0.8	0.644	0.615	0.623	0.635	0.651	0.737
1	0.769	0.739	0.750	0.764	0.782	0.901
2	1.50	1.47	1.49	1.52	1.55	1.82
3	2.44	2.42	2.45	2.49	2.52	2.94
4	3.59	3.58	3.60	3.67	3.71	4.27
5	4.94	4.93	4.96	5.05	5.10	5.80
6	6.48	6.47	6.49	6.62	6.67	7.53
7	8.19	8.19	8.21	8.38	8.42	9.46
8	10.07	10.07	10.09	10.31	10.35	11.58
9	12.12	12.13	12.15	12.41	12.45	13.88
10	14.33	14.35	14.38	14.68	14.72	16.38

b) complex

| Energy	Bone	Plagioclase	Pottery (sat)	Basalt	Pottery
0.01	0.021	0.027	0.027	0.027	0.027
0.05	0.074	0.099	0.099	0.101	0.101
0.1	0.118	0.157	0.156	0.161	0.161
0.15	0.154	0.203	0.202	0.208	0.208
0.2	0.186	0.244	0.242	0.251	0.250
0.3	0.242	0.317	0.313	0.326	0.324
0.4	0.293	0.384	0.378	0.395	0.391
0.6	0.387	0.511	0.501	0.525	0.520
0.8	0.479	0.637	0.624	0.653	0.648
1	0.575	0.766	0.751	0.785	0.782
2	1.15	1.52	1.5	1.56	1.56
3	1.92	2.48	2.47	2.55	2.57
4	2.87	3.66	3.64	3.75	3.78
5	4.00	5.03	5.01	5.15	5.2
6	5.28	6.58	6.57	6.75	6.8
7	6.72	8.32	8.31	8.53	8.6
8	8.3	10.22	10.23	10.48	10.57
9	10.04	12.3	12.31	12.61	12.72
10	11.92	14.55	14.57	14.91	15.05
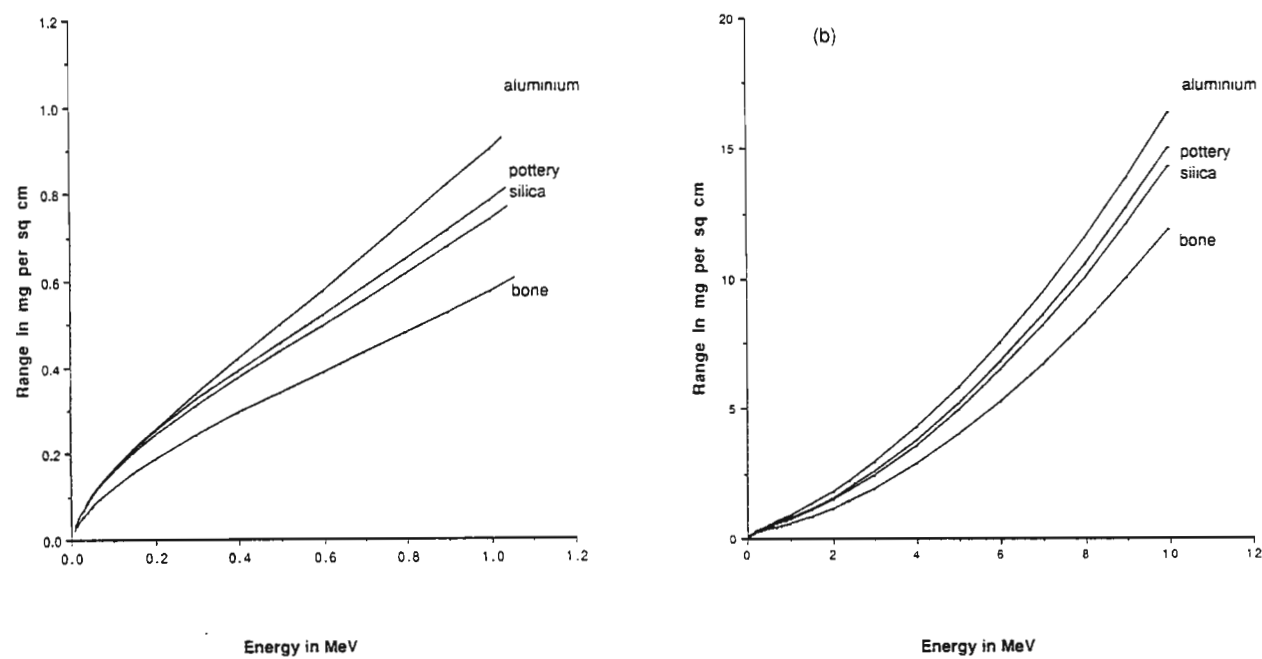
Figure 1.
Range as a function of energy for typical dating materials a) 0-1 MeV b) 0-10 MeV. Silica and dry pottery represent the extremes for most dating materials, except bone, with the majority lying closer to silica than pottery.

Table 2. Compositions, average atomic weights (A_{av}) and atomic numbers (Z_{av}) of dating materials used in calculating ranges. Note that, as the composition for pottery is highly variable, the values given for pottery are approximate only. Specific values, where required, must be derived from the actual composition of the sample. Compositions are in % by weight.

$$A_{av} = \left(\frac{\Sigma \, n_i \, A_i}{\Sigma \, n_i \, A_i^{0.5}} \right)^2 \qquad\qquad A_{av} = \left(\frac{\Sigma \, n_i \, Z_i}{\Sigma \, n_i \, Z_i^{0.5}} \right)^2$$

where n_i is the atomic abundance of the ith element.

Material	A_{av}	Z_{av}	Composition (% by weight)
Albite	20.1	10.2	$NaAlSi_3O_8$
Aluminium	27.0	13.0	Al
Anorthite	22.0	10.9	$CaAl_2Si_2O_8$
Basalt	22.8	11.3	SiO_2 (45), Al_2O_3 (14), FeO (10), Fe_2O_3 (3), MgO (11), CaO (10),Na_2O (3), TiO_2 (2), K_2O (1)
Bone	11.8	5.6	H (7), C (30), O (44), P (4), Ca (15)
Calcium carbonate	21.1	10.5	$CaCo_3$
Orthoclase	22.0	10.2	$KAlSi_3O_8$
Plagioclase	21.2	10.5	50% albite/50% anorthite
Pottery (dry)	23.1	11.3	SiO_2 (70), Al_2O_3 (15), Fe_2O_3 (5), K_2O (3), CaO (2), MgO (2), NaO (1), TiO_2 (1)
Pottery (sat.)	21.0	10.2	as above (93), H_2O(7) ie 15% porosity
Silica	20.4	10.2	SiO_2

Table 3.   Coefficients for polynomial approximations for deriving ranges in mg.cm^{-2} for alpha particles of different energies (MeV),
$$R = A_3E^3 + A_2E^2 + A_1E + A_0$$
Note that the constant term is negligible in the low energy polynomials as R = 0 for E = 0.
The corresponding equations for stopping powers may be calculated as the reciprocal of dR/dE.

Material	0 - 1 MeV			1 - 10 MeV			
	A_3	A_2	A_1	$A_3.10^3$	A_2	A_1	A_0
Albite	0.73	-1.28	1.29	-1.14	0.1107	0.422	0.22
Anorthite	0.72	-1.29	1.33	-1.26	0.1143	0.431	0.24
Basalt	0.75	-1.33	1.36	-1.37	0.1174	0.430	0.24
Bone	0.55	-1.00	1.01	-1.26	0.1012	0.286	0.19
Calc carb.	0.68	-1.26	1.33	-1.45	0.1160	0.391	0.26
Orthoclase	0.77	-1.36	1.34	-1.31	0.1158	0.416	0.23
Plagioclase	0.72	-1.29	1.31	-1.26	0.1135	0.423	0.23
Pottery	0.78	-1.37	1.35	-1.18	0.1152	0.448	0.22
Pottery (sat)	0.76	-1.33	1.31	-1.25	0.1140	0.420	0.22
Silica	0.76	-1.34	1.31	-1.36	0.1146	0.402	0.22

calculated. Valladas (1988) quotes linear expressions for dR/dE analogous to the expression 1+0.29E used by Zimmerman (1971). We note, however, that Zimmerman in fact assumed that dR/dE was proportional to (1 + 0.29E) , and, in the absence of the appropriate proportionality constants, the expressions quoted by Valladas do not provide useful estimates for dR/dE.

For silica, the ranges calculated using the 1988 implementation of Zeigler are 10 - 5 % percent smaller (for alpha energies from 3 - 10 MeV) than the ranges based on the data of Zeigler (1977), presented in Valladas (1988). In absolute terms the differences increase from 0.1 mg cm^{-2}, for 50 keV alphas through 0.31 mg cm^{-2} for 4 MeV alphas to 0.66 mg cm^{-2} for 10 MeV alphas. Differences are due largely to the updated data set and calculation method but the use of projected range instead of total range also makes a small contribution, reducing the ranges calculated by approximately 0.05 mg cm^{-2} (<1% for all alphas above 4 MeV).

Because the composition of pottery is highly variable, the difference between compositions used in range calculations may outweigh the effect of using different calculation methods. For example, the composition we used for dry pottery, which lay between the extremes we found in a brief literature search, gave us an A_{av} and Z_{av} of 23.1 and 11.3 (cf values of 21.4 and 10.6, respectively, in Bowman, 1982). Our higher values for A_{av} and Z_{av} were sufficient to offset the difference in calculation methods and coincidentally yielded very similar ranges to those cited in Aitken and Bowman (1985).

We have compared the different calculation methods, including one given in Benton and Henke (1969), by applying them to calcium carbonate (fig. 2). Note that the ranges derived by other methods are not simply proportional to the Zeigler (1988) ranges. The discrepancies are not large at the energies found in the natural environment, being generally less than 8%. At the energies below 1 MeV the differences are much more striking and may be important in estimating alpha doses due to external sources. It may reasonably be inferred that similar variations would also result from the application of the different methods to other materials.

Total ranges per parent disintegration for the uranium and thorium series, assuming equilibrium, in the various materials are given in table 4. Energies and branching ratios are taken from Nambi and Aitken (1986). The branching ratios in the Th-232 and U-235 chains have been applied to the ranges of the contributing alpha particles, not to the energies, as it is the average tracklength that is required, not the tracklength corresponding to the average energy. The difference in the two methods is small; averaging energies gives an underestimate of 1.5% for the branch in the Th-232 chain i.e. only 0.4% in the total Th-232 chain in equilibrium.

If dose rates are being calculated from range data, as in Aitken (1985), p287, the relevant data on total ranges from table 4 may be used to derive the average alpha ranges for lines 12 and 13 in Aitken's table G.4, for the specific material. The figures in lines 16-19 are then proportional to the appropriate alpha range.

The adjustments to natural dose rates implied by these revised estimates will generally be smaller than the uncertainty in the overall dating technique. Nevertheless, it is desirable to avoid systematic errors wherever possible by taking advantage of the most recent data and techniques.
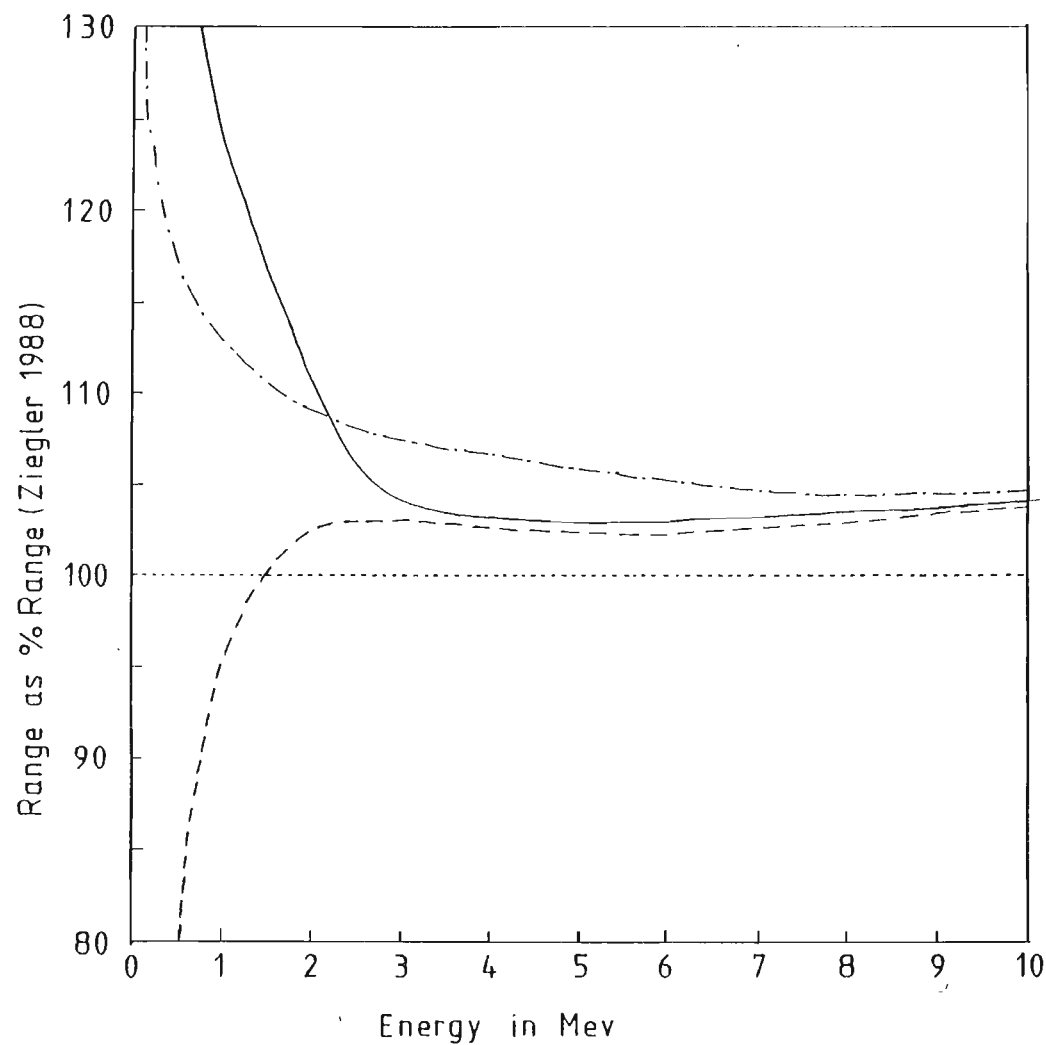
Figure 2.
Ranges for calcium carbonate calculated by various methods as a percentage of ranges calculated using Zeigler (1988), for alpha particle energies up to 10 MeV.

— . — . —   Zeigler 1977   - - - - - - - - - -   Benton and Henke

— — — — — —   Northcliffe and Schilling   ·················   Zeigler 1988

Table 4.   Total ranges in mg cm^{-2} for the uranium and thorium series in equilibrium. Values are per parent disintegration. Energy and branching ratio data is from Nambi and Aitken (1986). For a concentration of 1ppm by weight of natural uranium and thorium, the corresponding flux in a^{-1} cm^{-2} may be calculated by multiplying the total ranges by 389.7, 18.2, and 128.0 for U-238, U-235 and Th-232, respectively.

	CaCO$_3$	SiO$_2$	Albite	Ortho-clase	Anor-thite	Al	Bone	Plagio-clase	Pot (sat)	Basalt	Pot
Full chain											
U-238	44.56	44.47	44.64	45.54	45.90	52.03	36.17	45.29	45.18	46.43	46.81
U-235	45.28	45.22	45.39	46.30	46.61	52.63	36.92	46.01	45.93	47.18	47.26
Th-232	39.67	39.64	39.76	40.56	40.83	46.07	32.38	40.31	40.25	41.34	41.31
Pre-radon											
U-238	17.55	17.49	18.11	17.93	18.11	20.68	18.44	17.86	17.77	18.30	18.44
U-235	21.22	21.17	21.86	21.67	21.86	23.59	22.29	21.57	21.51	22.11	22.29
Th-232	15.08	15.05	15.55	15.41	15.55	17.68	15.86	15.34	15.30	15.73	15.86

References

Aitken, M.J., and Bowman, S.G.E. (1975) Thermoluminescence dating: assessment of alpha particle contribution *Archaeometry*, **17**, 132-138.

Benton, E.V., and Henke D.J. (1969) Heavy particle range-energy relations for dielectric nuclear track detectors *Nuclear instruments and methods* **67**, 87-92.

Bowman, S.G.E. (1982) Alpha particle range in pottery *PACT J.*, **6**, 61-66.

Lyons, R.G. (1988) Determination of alpha effectiveness in ESR dating using linear accelerator techniques: methods and energy dependence *Nuclear Tracks* **14** (1-2), 275-288.

Lyons, R.G., and Brennan, B.J. (1989) Values of η and keff/kref for alpha dose.rate calculations in speleothem calcite *Ancient TL*, **7(1)**, 1-4.

Lyons, R.G., and Brennan, B.J. (1989) Alpha effectiveness in ESR dating: energy dependence and implications for dose rate calculations *Int. Journ. Applied Radiation and Isotopes* (in press)

Marion, J.B., and Young, F.C. (1968) *Nuclear reactions analysis*. North Holland, Amsterdam.

Nambi, K.S.V., and Aitken, M.J. (1986) Annual dose conversion factors for TL and ESR dating *Archaeometry*, **28(2)**, 202-205.

Northcliffe, L.C., and Schilling, R.E. (1970) Range and stopping power for heavy ions. *Nuclear Data Tables* A7, 233- 463.

Valladas, G. (1988) Stopping power and range for alpha particles in SiO_2 *Ancient TL*, **6**, 1, 7-8.

Williamson, C.F., Boujod, J.P. and Picard, J. (1966) Tables of range and stopping power of chemical elements for charged particles of energy 0.05 to 500 MeV. Rapport CEA-R3042. Centre d'Etudes Nucleaires de Saclay.

Zimmerman, D.W. (1971) Thermoluminescent dating using fine-grains from pottery. *Archaeometry*, **13**, 29-52.

Zeigler, J.F. (1977) *Helium, stopping powers and ranges in all elemental matter*. Pergamon Press, Oxford.

Zeigler, J.F., Biersack, J.P., and Littmark, U. (1985) *The stopping and range of ions in solids* Vol 1 (ed Zeigler) Pergamon Press, New York.

PR Reviewer's comments (Martin Aitken)

It is good to see these definitive data on alpha ranges as well as on A_{av} and Z_{av} values; the latter will be useful in other contexts too. As the authors comment there is unlikely to be any significant shift in ages but it's reassuring to be on firmer ground.

Comparison between fine-grain and ultrathin TLD in the measurement of alpha dose-rate

Wang Weida[†], Xia Junding[†], and Zhou Zhixin [§]
[†]Research Laboratory, Shanghai Museum, 16 South Henan Road, Shanghai,China.
[§] Institute of Radiation Medicine, Shanghai Medical University, 2094 Zietu Road, Shanghai, China

Introduction

In our laboratory of TL dating, the palaeodose and the annual dose-rate are measured by fine-grain samples and ultrathin thermoluminescence dosimeters (TLD) respectively (Wang, 1983a, 1983b). The determination of internal dose-rates due to alpha and beta radiation in pottery using ultrathin TLD is quite convenient (Wang, 1983c), although TLD does not have the same geometry as the fine grains. Just as Aitken (1985) pointed out, since the thickness of the phosphor layer is about 10 μm, it might be expected that there would be significant attenuation of alpha dose-rate. Hence the question is whether the measured values of the alpha dose-rate are in good agreement with those using fine grains. If the two results are different, a correction may need to be made to the alpha dose-rate measured using ultrathin TLD. We have made a special study of this problem, the results from which are reported in this paper. Measurements of alpha and beta dose-rate using ultrathin TLD has been reported (Wang, 1983c).Here we describe the method of measurement of alpha dose-rate using fine-grain TLD.

Experimental

Sample preparation
Mix $CaSO_4$:Tm grains with the powdered sherd; their grain sizes should be the same, in the range 20-150 μm. The mixture is ground further in a ball mill, .producing a limited number of fine-grains. The samples used in the study and laced in this manner are given in table 1.

Experimental Method
The laced samples and several ultrathin TLD were annealed for 60 mins at 400 °C, after which the ultrathin TLD were put into a glass container with the laced sample according to Wang's method (1983c). Hence the (beta-equivalent) annual alpha dose, D_α, and beta plus gamma annual dose, $D_{\gamma+\beta}$, are obtained by two equations,

$$D_\alpha = \frac{2 \, (\, D_a - D_b \,)}{t} \qquad (1)$$

$$D_{\beta+\gamma} = \frac{D_b}{t} \qquad (2)$$

where,
D_a and D_b are respectively the average dose of type a and b dosemeters, t is the storage time in years, and γ

denotes the environmental background (for further details, see Wang, 1983c) [†].

After withdrawal of the ultra-thin TLD, the fine grain discs were made from the laced sample. The fine-grain samples on the discs contain both $CaSO_4$:Tm and pottery powder. However the TL contribution from the pottery powder is negligible because its sensitivity is very much lower than the $CaSO_4$:Tm. The annual equivalent beta dose of the disc sample, D_F, is given by

$$D_F = \frac{D_f}{t} \qquad (3)$$

where D_f is the equivalent beta dose for the disc sample. The (beta equivalent) annual alpha dose for the disc sample, D'_α is also obtained by the equation

$$D'_\alpha = D_F - D_{\beta+\gamma} \qquad (4)$$

In equation (4) we assume that the measurement of $D_{\beta+\gamma}$ is reliable using the ultrathin TLD method. If $D_\alpha = D'_\alpha$, we consider that the ultrathin TLD method is also reliable in measurement of alpha dose-rate. If not, a correction must be made for the ultrathin TLD method. It should be noted that all the dose-rates measured using the two methods are standardized to an identical laboratory beta source. Hence the calibration error of the beta source is not important.

Results and discussion

Tables 2.1 and 2.2 give the comparison between fine-grain and ultrathin TLD of measured of alpha dose-rate. Tables 2.1 and 2.2 show that the ultrathin TLD is $8.5 \pm 4.9\%$ less efficient in measurement of alpha dose-rate than the fine-grain TLD method when using 2 mg cm^{-2}, and is $2.8 \pm 5.2\%$ less when using 1 mg cm^{-2}. A comparison between the neutron activation analysis (NAA) and ultrathin TLD is given in tables 3 and 5 (laced samples) and tables 4 and 6 (ancient pottery and bricks).
The alpha dose-rate given represents the beta-equivalent dose-rate, and k is the ratio of alpha to beta sensitivity; k = 0.29 (±3%) for 1 mg cm^{-2} and 0.27

[†]*Ed. note.*
From Wang's 1982 paper, the construction of each type of dosemeter is as follows:
Type a - phosphor deposited onto 8 mm diameter, 10 μm thick aluminium foil to a thickness of 2 mg cm^{-2}.
Type b - as type a with a layer of foil covering the phosphor surface ie completely shielded from alpha particles.

($\pm 3\%$) for 2 mg cm^{-2}. Tables 3 and 5 show that as long as different values of k are used, the ultrathin TLD of different thicknesses give the same alpha dose-rate. In fact, the k value acts as a compensator for thickness. The k-value was calibrated by using New Brunswick Laboratory samples (No.109 and No.105) containing respectively, 0.01% of thorium series and 0.001% of uranium series in silica, provided by the Oxford Laboratory and calculated according to

$$k = \frac{2 (D_a - D_b)}{(t \, D_{\alpha o})} \quad (5)$$

where $D_{\alpha o}$ is the alpha dose-rate for NBL samples according to their specified contents of thorium and uranium.

Tables 3 and 4 show that the ultrathin TLD results are in reasonable agreement with NAA; conversely, the alpha dose-rate is obviously decreased if the k-value of 0.29 is used for a TLD thickness of 2 mg cm^{-2}. The measurement of beta dose-rate is also shown in table 4.

Even so, the ultrathin results still have a tendency to be less than the NAA results. The difference arises from two factors:

1. The NAA method involves the assumption of equilibrium of long-lived radionuclides. In fact, the equilibrium cannot be assumed for younger clay sediments. The TLD method measures the dose-rate for the state of disequilibrium under present conditions; therefore, the TLD method is more reliable than the NAA method.

2. As mentioned above, using TLD of 1 mg cm^{-2} the measured alpha dose-rate was 2.8% less than with NAA; perhaps it is one of the reasons giving rise to the differences between the two methods. Nonetheless, the experimental results show that ultrathin TLD enables measurement of alpha dose-rate, providing the thickness of phosphor on the aluminium foil is less than the least alpha particle range. The phosphor thickness for the ultrathin TLD of 1 mg cm^{-2} is about a few microns, and it can be penetrated by nearly all alpha particles. But for the ultrathin TLD of thickness 2 mg cm^{-2}, a correction is necessary; however the correction is included in the k-value.

If the aim is only to date, it is unnecessary to make excessive demands concerning the size of the phosphor grains. Because the age equals the ratio of palaeodose to annual dose (providing the size of fine grains of the archaeological sample and the phosphor are the same) the palaeodose and the annual dose suffer the same attenuation and there is no influence on the determined age.

References
Aitken, M. J. (1985) *Thermoluminescence Dating*. Academic Press, London, p 112.
Wang, W., and Zhou, Z. (1983a) Thermoluminescence dating of Chinese pottery. *Archaeometry*, **25(2)**, 99-106.
Wang, Weida (1983b) A study on thermoluminescence dating: all measurement are made by using TLD. *Nuclear Electronics and Detection Technology*, **3(4)**, 1-11 (in Chinese).
Wang, Weida (1983c) Ultrathin TLD measurement of alpha dose-rate and comparison with alpha counting. *Ancient TL*, **1(1)**, 2-4.

PR. Reviewer's comments (M. J. Aitken)
This note follows on from the pottery dating procedure described by Wang and Zhou (1983), a procedure which is evidently in routine use at the Shanghai Museum. Because the annual dose is assessed by phosphor dosimetry it has the strong advantage that the dates obtained do not depend on radioactive source calibration, at any rate to first order. The present note investigates the question of how thin the ultrathin phosphor film must be in order to avoid significant attenuation of alpha particles; it is good news that for a thickness of 1 mg cm^{-2} there is no significant attenuation (to within $\pm 5\%$ experimental error).

Table 1.   Composition of experimental samples

Lab. No.	Source of sherds	$CaSO_4$:Tm content, %
10	Songze site, Qingpu County, Shanghai	30
11	Fuquanshan site, Qingpu County, Shanghai	40
12	Fuquanshan site, Qingpu County, Shanghai	45
14	Tinglin site, Jinshan County, Shanghai	50

Table 2.1 Comparison of alpha dose-rate measurements obtained using fine-grain and ultrathin (2 mg cm^{-2}) TLD methods

No.	Alpha dose-rate (beta equivalent)		$\dfrac{D'_\alpha - D_\alpha}{D'_\alpha}$
	D'_α fine-grain	D_α ultrathin	
	mGy/a	mGy/a	%
10	5.44 ± 0.05	4.82 ± 0.27	+11.0 ± 4.9
	5.06 ± 0.05	4.69 ± 0.29	+7.3 ± 5.8
	5.33 ± 0.08	5.02 ± 0.20	+5.8 ± 4.0
	5.25 ± 0.06	4.77 ± 0.20	+9.1 ± 4.0
Average	5.27 ± 0.06	4.83 ± 0.24	+8.3 ± 4.7
11	5.09 ± 0.07	4.69 ± 0.18	+7.9 ± 3.8
	4.79 ± 0.09	4.48 ± 0.17	+6.5 ± 4.0
	4.96 ± 0.07	4.32 ± 0.32	+11.3 ± 6.7
	5.29 ± 0.12	4.81 ± 0.19	+9.1 ± 4.3
Average	5.03 ± 0.09	4.58 ± 0.22	+8.9 ± 4.7
12	3.99 ± 0.09	3.55 ± 0.21	+11.0 ± 5.7
	3.62 ± 0.05	3.28 ± 0.14	+9.4 ± 4.1
	4.03 ± 0.12	3.81 ± 0.23	+5.5 ± 6.5
	4.30 ± 0.08	4.02 ± 0.18	+6.5 ± 4.6
	4.10 ± 0.05		
	3.78 ± 0.03		
Average	3.97 ± 0.07	3.67 ± 0.19	+7.6 ± 5.1
14	3.97 ± 0.06	3.74 ± 0.13	+5.8 ± 3.6
	4.17 ± 0.10	3.82 ± 0.21	+8.4 ± 5.6
	3.73 ± 0.05	3.44 ± 0.17	+7.8 ± 4.8
	3.80 ± 0.06	3.29 ± 0.22	+13.0 ± 5.8
	3.68 ± 0.07		
	4.15 ± 0.09		
	4.01 ± 0.11		
Average	3.93 ± 0.08	3.57 ± 0.18	+9.2 ± 5.0

Average for 4 groups = + 8.5 ± 4.9 %

Table 2.2 Comparison of alpha dose-rate measurements obtained using fine-grain and ultrathin (1 mg cm^{-2}) TLD methods.

No.	Alpha dose-rate (beta equivalent)		$\dfrac{D'_\alpha - D_\alpha}{D'_\alpha}$
	D'_α fine-grain	D_α ultrathin	
	mGy/a	mGy/a	%
10		4.96 ± 0.20	+5.9 ± 4.0
		5.04 ± 0.26	+4.4 ± 5.1
		5.31 ± 0.32	-0.76 ± 6.0
Average	5.27 ± 0.06	5.10 ± 0.26	+3.2 ± 5.0
11		4.93 ± 0.19	+2.0 ± 4.2
		4.61 ± 0.27	+8.3 ± 5.6
Average	5.03 ± 0.09	4.77 ± 0.23	+5.2 ± 4.9
12		3.74 ± 0.25	+5.8 ± 6.5
		4.08 ± 0.19	-2.8 ± 5.2
		3.88 ± 0.12	+2.3 ± 3.6
		4.22 ± 0.21	-6.3 ± 5.6
Average	3.97 ± 0.07	3.98 ± 0.19	-0.25 ± 5.1
14		3.77 ± 0.15	+4.1 ± 4.4
		3.82 ± 0.18	+2.9 ± 5.2
		4.10 ± 0.27	-4.3 ± 7.1
		3.53 ± 0.23	+1.0 ± 6.1
Average	3.93 ± 0.08	3.81 ± 0.21	+3.1 ± 5.8

Average for 4 groups = + 2.5 ± 5.2 %

Table 3. Comparison of fine grain, ultrathin TLD and NAA methods for measurement of alpha dose-rate.

No.	Fine-grain k =0.29	Ultrathin TLD 1 mg.cm^{-2} k=0.29	Ultrathin TLD 2 mg.cm^{-2} k=0.27	Ultrathin TLD 2 mg.cm^{-2} k=0.29	NAA
10	18.17 ± 0.21	17.59 ± 0.90	17.89 ± 0.89	16.66 ± 0.83	17.56 ± 0.67
11	17.34 ± 0.31	16.45 ± 0.79	16.96 ± 0.81	15.79 ± 0.76	18.71 ± 0.69
12	13.69 ± 0.24	13.72 ± 0.65	13.59 ± 0.70	12.66 ± 0.66	15.44 ± 0.56
14	13.55 ± 0.28	13.14 ± 0.72	13.22 ± 0.67	12.31 ± 0.62	14.01 ± 0.49

Alpha dose-rate, mGy a^{-1}

Table 4. Comparison; measurement of alpha dose-rate in ancient pottery and bricks using ultrathin TLD and NAA methods.

No.	Alpha dose-rate Ultrathin TLD 2 mg.cm^{-2}	Alpha dose-rate NAA	Beta dose-rate Ultrathin TLD 2 mg.cm^{-2}	Beta dose-rate NAA
SB 185	22.65 ± 1.31	23.11 ± 0.79	2.20 ± 0.05	2.46 ± 0.09
SB 186	23.10 ± 1.55	24.39 ± 0.95	2.77 ± 0.11	2.51 ± 0.09
SB 191	15.98 ± 1.11	17.51 ± 0.58	2.56 ± 0.13	2.44 ± 0.09
SB 192	18.35 ± 1.10	18.10 ± 0.58	2.49 ± 0.07	2.33 ± 0.08
SB 193	22.23 ± 1.18	21.50 ± 0.75	2.89 ± 0.05	3.28 ± 0.11
SB 203	17.95 ± 1.08	18.23 ± 0.71	2.31 ± 0.04	2.51 ± 0.10
SB 204	17.68 ± 1.29	18.37 ± 0.65	2.34 ± 0.06	2.12 ± 0.07
SB 205	14.49 ± 1.88	17.68 ± 0.60	2.15 ± 0.21	2.32 ± 0.09
SB 206	27.42 ± 1.51	29.89 ± 1.02	2.32 ± 0.06	2.13 ± 0.10
SB 207	20.15 ± 0.99	19.64 ± 0.69	3.28 ± 0.08	3.06 ± 0.11

mGy a^{-1}

Table 5. The ratio of TLD/NAA for alpha dose-rate measurement

No.	Fine-grain k_{TLD}=0.29	1 mg.cm^{-2} k_{TLD}=0.29	Ultrathin TLD 2 mg.cm^{-2} k_{TLD}=0.27	2 mg.cm^{-2} k_{TLD}=0.29
10	1.03 ± 0.04	1.00 ± 0.06	1.02 ± 0.06	0.95 ± 0.06
11	0.93 ± 0.04	0.88 ± 0.05	0.91 ± 0.05	0.84 ± 0.05
12	0.89 ± 0.04	0.89 ± 0.05	0.88 ± 0.06	0.82 ± 0.05
14	0.97 ± 0.04	0.94 ± 0.06	0.94 ± 0.06	0.88 ± 0.05
Average	0.96 ± 0.04	0.93 ± 0.06	0.94 ± 0.06	0.87 ± 0.05

Table 6. The ratio of TLD/NAA measurement of alpha and beta dose-rate in archaeological samples

No.	TLD/NAA (Ultrathin TLD: 2 mg cm^{-2}, k_{TLD} = 0.27) Alpha dose-rate	Beta dose-rate
SB 185	0.98 ± 0.07	0.89 ± 0.04
SB 186	0.95 ± 0.07	1.10 ± 0.06
SB 191	0.91 ± 0.07	1.05 ± 0.07
SB 192	1.01 ± 0.07	1.07 ± 0.05
SB 193	1.03 ± 0.07	0.88 ± 0.03
SB 203	0.98 ± 0.07	0.92 ± 0.04
SB 204	0.96 ± 0.08	1.10 ± 0.05
SB 205	0.82 ± 0.11	0.93 ± 0.10
SB 206	0.92 ± 0.06	1.09 ± 0.05
SB 207	1.03 ± 0.06	1.07 ± 0.05
Average	0.96 ± 0.07	1.01 ± 0.05

Bibliography

Berger, G.W. (1989) Comment on the present status of dating loess by thermoluminescence. In *Late Cenozoic History of the Interior Basins of Alaska and the Yukon.* (eds. L.D. Carter, T.D. Hamilton and J.P Galloway). USGS Circular 1026, 103-105.

Berger, G.W. (1988) Dating Quaternary events by luminescence. Geological Soc. of America Special Paper 227, 13-50.

Cini Castagnoli, G., Bonino, G. and Provenzale, A. (1988) The thermoluminescence profile of a recent sea sediment core and the solarvariability. *Solar Physics,* **117**, 187-197.

Forman, S.L., Machette, M.N., Jackson, M.E. and Maat, P. (1989) An evaluationof thermoluminescence dating of paleoearthquakes on the American Fork segment,Wasatch fault zone, *Utah Journal of Geophysical Research,* **94**, 1622-1630.

Grün, R. (1989) ESR dating for the early Earth. *Nature,* **338**, 543-544.

Hornyak, W.F. and Franklin, A.D. (1988) A second-generation 3-D spectrophotometer for TL analysis. *Journal of Luminescence,* **42**, 89-96.

Jungner, H., Lanvik, J.Y. and Mangerud, J. (1989) Thermoluminescence dates of Weichselian sediments in western Norway. *Boreas,* **18**, 23-29.

Odom, A.L. and Rink, W.J. (1989) Natural accumulation of Schottkey-Frenkel defects: implications for a quartz chronometer. *Geology,* **17**, 55-58.

Prescott, J.R., Fox, P.J., Akber, R.A. and Jensen, H.E. (1988) Thermoluminescence emission spectrometer. *Applied Optics,* **27**, 3496-3502.

Rögner, K., Löscher, M. and Zöller, L. (1988) Stratigraphie, Palaogeographie und erste Thermolumineszenz datierungen in der westlichen Iller-Lech-Platte (nordliches Alpenvorlan d, Deutschland). *Z. Geomorph. N.F.,* **70**, 51-73.

Schwarcz, H.P., Grün, R., Vandermeersch, B., Bar-Yosef, O.,Valladas, H., and Tchernov, E. (1988) ESR dates for the hominid burial site of Qafzeh in Israel. *Journal of Human Evolution,* **17**, 733-737.

Singhvi, A.K., Bronger, A., Sauer, W. and Pant, R.K. (1989) Thermoluminescence dating of loess-paleosol sequences in the Carpathian Basin (east-central Europe): a suggestion for a revised chronology. *Chemical Geology,* **73**, 307-317.

Stringer, C.B., Grün, R., Schwarcz, H.P., and Goldberg, P. (1989) ESR dates on the hominid burial site of Es Skul in Israel. *Nature,* **338**, 756-758.

TL dates reported in:
Olsen, L. (1988) Stadials and interstadials during the Weichsel glaciation in Finnmarksvidda, northern Norway. *Boreas,* **17**, 517-539.

ESR dates reported in:
Jacobson, G., Arakel, A.V., and Chen, Y.J. (1988) The central Australian groundwater discharge zone: evolution of associated calcrete and gypsum deposits. *Australian Journal of Earth Sciences,* **35**, 549-565.

Compiled by Ann Wintle